Materials Research. 2018; 21(5): e20180173
DOI: http://dx.doi.org/10.1590/1980-5373-MR-2018-0173

Kinetics of Formation of Fe_2B Layers on AISI S1 Steel

Jorge Zuno- Silva[a], Mourad Keddam[b]*, Martin Ortiz-Domínguez[a], Milton Carlos Elias-Espinosac[c], Felipe Cervantes- Sodi[d], Joaquín Oseguera-Peña[e], Libia Daniella Fernández De- Dios[f], Oscar Armando Gomez-Vargas[f]

[a]Escuela Superior de Ciudad Sahagún-Ingeniería Mecánica, Universidad Autónoma del Estado de Hidalgo, Carretera Cd. Sahagún-O tumba s/n, Zona Industrial CP. 43990, Hidalgo, México
[b]Laboratoire de Technologie des Matériaux, Faculté de Génie Mécanique et Génie des Procédés, Université des Sciences et de la Technologie Houari Boumediene - USTHB, B.P. No. 32, 16111 El-Alia, Bab-Ezzouar, Algiers, Algeria
[c]Tecnológico de Monterrey-Campus Santa Fe, Av. Carlos Lazo No. 100, Del. Álvaro Obregón, CP. 01389, México City, México
[d]Departamento de Física y Matemáticas, Universidad Iberoamericana, Ciudad de México, Prolongación Paseo de la Reforma 880, Lomas de Santa Fe, CP. 01219, México City, México
[e]Tecnológico de Monterrey, Campus Estado de México, Av. Lago de Guadalupe KM 3.5. Col. Margarita Maza de Juárez, Atizapán de Zaragoza, CP. 52926, Edo. De Méx., México
[f]Instituto Tecnológico de Tlalnepantla-ITTLA, S/N. Col. La Comunidad, Tlalnepantla de Baz, CP. 54070, Estado de México, México

Received: March 07, 2018; Revised: April 25, 2018; Accepted: June 05, 2018

In the present work, the AISI S1 steel was pack-borided in the temperature range 1123-1273 K for 2- 8 h to form a compact layer of Fe_2B at the material surface. A recent kinetic approach, based on the integral method, was proposed to estimate the boron diffusion coefficients in the Fe_2B layers formed on AISI S1 steel in the temperature range 1123-1273 K. In this model, the boron profile concentration in the Fe_2B layer is described by a polynomial form based on the Goodman's method. As a main result, the value of activation energy for boron diffusion in AISI S1 steel was estimated as 199.15 $kJmol^{-1}$ by the integral method and compared with the values available in the literature. Three extra boriding conditions were used to extend the validity of the kinetic model based on the integral method as well as other diffusion models. An experimental validation was made by comparing the values of Fe_2B layers' thicknesses with those predicted by different diffusion models. Finally, an iso-thickness diagram was proposed for describing the evolution of Fe_2B layer thickness as a function of boriding parameters.

Keywords: *Incubation time, Diffusion models, Activation energy, Growth kinetics, Integral method.*

1. Introduction

The boriding process is a thermochemical treatment in which the boron atoms are diffused into the surface of a workpiece to form hard layers composed of iron borides and metallic boride in the case of high alloy steels[1]. For carbon steels, two kinds of iron borides can be formed by boriding in the temperature range 800-1050°C.

The iron borides are interesting phases because of their high hardness. Nevertheless, the Fe_2B phase is preferred to FeB, when the resistance to wear under impact was required, since the doublé boride layer (FeB and Fe_2B) is prone to cracking during service. Among the boriding processes, the powder-pack boriding is widely used in the industry because of its easy handling and low cost[2]. In this boriding method, a mixture of powders that consists of a boron yielding substance, an activator and a diluent is used. The samples to be borided are then packed in a stainless steel container and placed in the furnace.

In the literature, no kinetic study was reported on the boriding of AISI S1 steel. The modeling of boriding process can be used as a tool to optimize the boriding parameters to produce boride layers with sufficient thicknesses that meet the requirements during service life.

From a kinetic point of view, several approaches have beeen developed to study the kinetics of formation of Fe_2B layers on Armco iron and steels as substrates[3-12].

All these diffusion models considered the principle of the mass balance equation at the (Fe_2B/substrate) interface under certain assumptions (with and without boride incubation times).For instance, Ortiz-Domínguez et al.[5] have developed a kinetic model for studying the growth kinetics of Fe_2B layers on gray cast iron by introducing a kinetic parameter that depends on the values of upper and lower boron concentrations in Fe_2B and on the boride incubation time.Elias-Espinosa et al.[6] have modeled the growth kinetics of Fe_2B layers on AISI O1 steel by using a diffusion model that assumes a nonlinear boron concentration profile with the presence of

*e-mail: keddam@yahoo.fr

a constant boride incubation time. They have introduced a non dimensional kinetic parameter to evaluate the boron diffusion coefficients in the Fe_2B layers in the temperature range 1123-1273 K. Similarly, Nait Abdellah et al.[7] have also suggested a kinetic model based on the mass balance equation at the (Fe_2B/Fe) interface by assuming a nonlinear boron concentration profile through the Fe_2B layers on Armco substrate. They introduced the β(T) parameter that depends on the boriding temperature. Flores-Rentería et al.[8] have modelled the kinetics of formation of Fe_2B layers on AISI 1026 steel by using a kinetic model. In their model, they introduced a kinetic parameter called ε which is independent on the boriding temperature with a linear boron concentration profile in the Fe_2B layer.

In the present study, a recent kinetic approach based on the integral method [3,4] has been suggested to investigate the boriding kinetics of AISI S1 steel by taking into account the presence of boride incubation time.

The aim of the present work was to investigate the growth kinetics of Fe_2B layers on AISI S1 steel based on the integral method in the temperature range 1123-1273 K.

This diffusion problem can be solved either analytically or numerically.An analytic solution for the integral method has been obtained in order to estimate the boron diffusion coefficients in Fe_2B. An experimental validation of the integral method and other used diffusion models was also made for an upper boron concentration of 9 wt.% in Fe_2B.Furthermore, the value of activation energy for boron diffusion in AISI S1 steel was estimated on the basis of the integral method and compared with that obtained from another diffusion model [6]. Finally, the estimated value of boron activation energy from the integral method was compared with the data available in the literature.

2. The Diffusion Model

The diffusion model deals with the growth kinetics of Fe_2B layer on a saturated matrix with boron atoms. The boron concentration- profile along the Fe_2B layer is depicted in Figure 1.

The f(x,t) function shows the distribution of boron concentration within the substrate before the formation of Fe_2B phase $t_0^{Fe_2B}$ *(T)* represents the boride incubation time required to form a compact and continuous Fe_2B layer. $C_{up}^{Fe_2B}$ is the upper limit of boron content in Fe_2B (=9 wt.%) while $C_{low}^{Fe_2B}$ represents the lower limit of boron content in Fe_2B(=8.83wt.%).The variable x(t)=u is the position of (Fe_2B/substrate) interface. A small homogeneity range of about 1 at. % was observed by Brakman et al.[13] for the Fe_2B layer. The term C_{ads}^{B} is the adsorbed boron concentration in the boride layer during the boriding treatment[14]. C_0 represents the boron concentration in the substrate of a very low solubility (≈0 wt.%)[15-17].

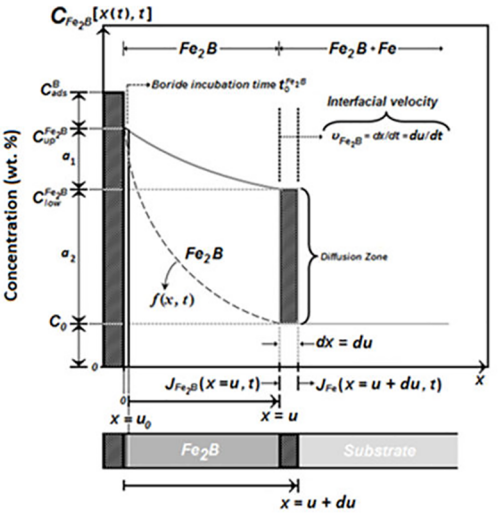

Figure 1. Schematic representation of the boron-concentration profile through the Fe_2B layer

The assumptions taken into account during the formulation of integral model are given in the reference works [3,4]:

The initial and boundary conditions for the diffusion problem are given by:

$$t=0, x>0, \text{ with } C_{Fe_2B}[x(t), t=0] = C_0 \approx 0 \text{ wt..\%} \quad (1)$$

Boundary conditions:

$$C_{Fe_2B}[x(t=t_0^{Fe_2B})=0, t=t_0] = C_{up}^{Fe_2B} \text{ for } C_{ads}^{B} > 8.83\text{wt.\%} \quad (2)$$

$$C_{Fe_2B}[x(t=t)=u(t), t=t] = C_{low}^{Fe_2B} \text{ for } C_{ads}^{B} < 8.83\text{wt.\%} \quad (3)$$

The Second Fick's law describing the change in the boron concentration within the Fe_2B layer is given by Equation (4):

$$D_{Fe_2B}\frac{\partial^2 C_{Fe_2B}[x,t]}{\partial x^2} = \frac{\partial C_{Fe_2B}[x,t]}{\partial t} \quad (4)$$

$C_{Fe_2B}[x,t]$ is the distribution of boron element within Fe_2B layer (wt.%) and D_{Fe_2B} represents the diffusion coefficient of boron in the Fe_2B phase. The boron-concentration profile along the Fe_2B layer was described by the Goodman'smethod[17] as follows:

$$C_{Fe_2B}[x,t] = C_{low}^{Fe_2B} + a(t)(u(t)-x) + b(t)(u(t)-x)^2 \text{ for } 0 \le x \le u \quad (5)$$

The three time-dependent unknowns a(t), b(t) and u(t) have to meet the boundary conditions given by Equations (2) and (3). By applying the boundary condition on the surface, Equation (6) was obtained:

$$a(t)u(t)+b(t)u(t)^2=\left(C_{up}^{Fe_2B}-C_{low}^{Fe_2B}\right) \quad (6)$$

By integrating Equation (4) between 0 and u(t) and applying the Leibniz rule, the ordinary differential equation (ODE) given by Equation (7) was derived:

$$\frac{u(t)^2}{2}\frac{da(t)}{dt}+a(t)u(t)\frac{du(t)}{dt}+\frac{u(t)^3}{3}\frac{db(t)}{dt}+b(t)u(t)^2\frac{du(t)}{dt}=2D_{Fe_2B}b(t)u(t) \quad (7)$$

The mass balance equation at the (Fe_2B/substrate) interface can be formulated by Equation (8):

$$W\frac{dx}{dt}\bigg|_{x=u}=-D_{Fe_2B}\frac{\partial C_{Fe_2B}[x,t]}{\partial x}\bigg|_{x=u} \quad (8)$$

With $W=\left[\frac{C_{up}^{Fe_2B}-C_{low}^{Fe_2B}}{2}+\left(C_{low}^{Fe_2B}-C_0\right)\right]$

At the (Fe_2B/substrate) interface, the boron concentration remains constant and Equation (8) can be rewritten as follows:

$$W\left(-\frac{\frac{\partial C_{Fe_2B}[x,t]}{\partial t}\Big|_{x=u}}{\frac{\partial C_{Fe_2B}[x,t]}{\partial x}\Big|_{x=u}}\right)=-D_{Fe_2B}\frac{\partial C_{Fe_2B}[x,t]}{\partial x}\bigg|_{x=u} \quad (9)$$

Substituting Equation (4) into Equation (9) and after derivation with respect to the diffusion distance x(t), Equation (10) was deduced:

$$\left(C_{up}^{Fe_2B}+C_{low}^{Fe_2B}\right)b(t)=a(t)^2 \quad (10)$$

Equations (6), (7) and (10) constitute a set of differential algebraic equations (DAE) in a(t), b(t) and u(t) subjected to the initial conditions of this diffusion problem. To obtain the expression of boron diffusion coefficient in the Fe_2B layers, an analytic solution is possible by setting:

$$u(t)=k\left[t-t_0^{Fe_2B}(T)\right]^{1/2} \quad (11)$$

$$a(t)=\frac{\alpha}{u(t)} \quad (12)$$

and

$$b(t)=\frac{\beta}{u(t)^2} \quad (13)$$

where u(t) is the Fe_2B layer thickness and k the corresponding parabolic growth constant at the (Fe_2B/substrate) interface. The two unknowns α and β which are positive have to be searched for solving this diffusion problem. After substitution of Equations (11), (12) and (13) into the DAE (differential algebraic equations) system and derivation, the expression of boron diffusion coefficient was obtained as follows:

$$D_{Fe_2B}=\eta k^2 \quad (14)$$

where η is a dimensionless parameter.
with

$$\eta=\left[\left(\frac{1}{16}\right)\left(\frac{C_{up}^{Fe_2B}+C_{low}^{Fe_2B}}{C_{up}^{Fe_2B}-C_{low}^{Fe_2B}}\right)\left(1+\sqrt{1+4\left(\frac{C_{up}^{Fe_2B}-C_{low}^{Fe_2B}}{C_{up}^{Fe_2B}+C_{low}^{Fe_2B}}\right)}\right)+\left(\frac{1}{12}\right)\right]$$

along with the expressions of a(t) and b(t) given by Equations (15) and (16):

$$a(t)=\frac{\alpha}{k\left[t-t_0^{Fe_2B}(T)\right]^{1/2}} \quad (15)$$

$$b(t)=\frac{\beta}{k^2\left[t-t_0^{Fe_2B}(T)\right]} \quad (16)$$

With $\alpha=\frac{\left(C_{up}^{Fe_2B}+C_{low}^{Fe_2B}\right)}{2}\left[-1+\sqrt{1+4\left(\frac{C_{up}^{Fe_2B}-C_{low}^{Fe_2B}}{C_{up}^{Fe_2B}+C_{low}^{Fe_2B}}\right)}\right]$

and

$$\beta=\frac{\left(C_{up}^{Fe_2B}+C_{low}^{Fe_2B}\right)}{4}\left[2+4\left(\frac{C_{up}^{Fe_2B}-C_{low}^{Fe_2B}}{C_{up}^{Fe_2B}+C_{low}^{Fe_2B}}\right)-2\sqrt{1+4\left(\frac{C_{up}^{Fe_2B}-C_{low}^{Fe_2B}}{C_{up}^{Fe_2B}+C_{low}^{Fe_2B}}\right)}\right]$$

3. Experimental Details

3.1 The material and the boriding treatment

The AISI S1 steel was used as substrate for the powder-pack boriding. The chemical composition of AISI S1 steel is listed (in weight percent) in Table 1.

The samples had a cubic shape with nominal dimensions of 10 mm×10 mm×10 mm. Before the boriding treatment, the samples were cut and the cross-sections were polished

Table 1. The chemical composition of AISI S1 steel (in weight percent).

C	Mn	Si	Cr	Mo	W
0.40-0.55	0.10-0.40	0.15-1.20	1.00-1.80	0.35-0.50	1.50-3.00
V	Ni	Cu	P	S	Fe
0.15-0.30	0.3	0.25	0.03	0.03	balance

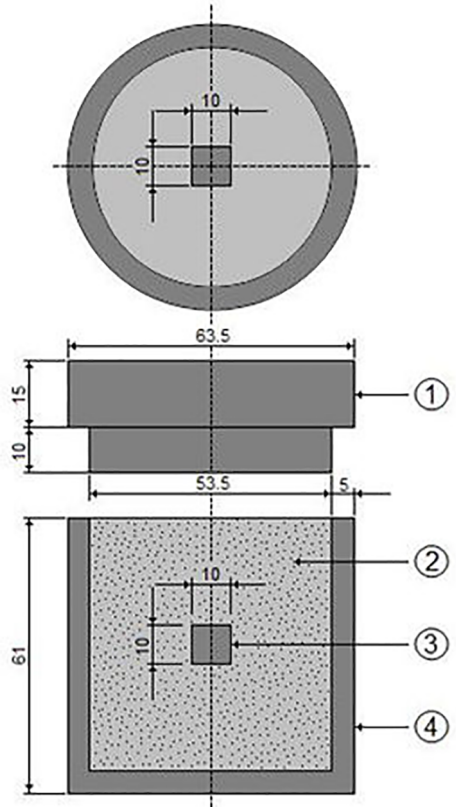

Figure 2. Schematic view of the stainless steel AISI 304L container for the pack-powder boriding treatment (1: lid; 2: powder boriding medium (B_4C + KBF_4 + SiC); 3: sample; 4: container)

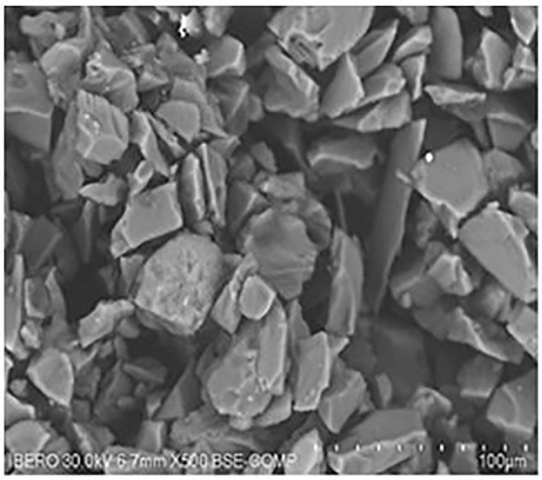

Figure 3. SEM image of boriding agent containing three components B_4C, KBF_4 and SiC

metallographically and then etched by Nital solution to reveal the microstructure. The powder-pack boriding was carried out by embedding the samples in a closed-container containing a mixture of powders as shown in Figure 2. The used boriding agent was composed of 20% B_4C, 10% KBF_4 and 70% SiC. Figure 3 gives an SEM image of the mixture of powders having an average size of 30 µm.

The container was placed in a conventional furnace under a pure argon atmosphere in the temperature range 1123-1223 K. Four treatment times (2, 4, 6 and 8 h) were selected for each temperature. Once the boriding treatment was finished the container was removed from the furnace and slowly cooled to room temperature.

3.2 Experimental techniques

The cross-sections of formed boride layers were examined by SEM (JEOL JSM 6300 LV). The boride layer thickness was automatically measured by means of MSQ PLUS software. For the reproducibility of measurements, seventy tests were performed from a fixed reference on different sections of borided samples to estimate the Fe_2B layer thickness; defined as an average value of the long boride teeth. The presence of the iron boride formed at the surface of treated sample was verified by use of X-Ray Diffraction (XRD) equipment (Equinox 2000) with Co-Kα radiation of wavelength λ_{Co} = 0.179 nm.

4. Results and Discussions

4.1 SEM examinations of Fe_2B layers

Figure 4 shows the cross-sections of borided samples at a temperature of 1173 K for different treatment times (2, 4, 6 and 8 h). It is seen the formation of a dense and compact Fe_2B layer with a peculiar morphology. The SEM pictures revealed the presence of a saw-tooth morphology. Such morphology is typical for borided Armco iron and carbon steels where as for high alloy steels the obtained morphology is very different. In fact, when increasing the contents of alloying elements the interface (boride layer/substrate) interface tends to be flat as observed, for example, in the pack-borided AISI 316 L steel[18]. Carbucicchio et al.[19] explained the occurrence of a saw-tooth morphology to the enhanced growth at the tips of boride needles. Consequently, the iron borides developed a textured growth along the preferred crystallographic direction [001] after Palombarini et al.[20].

The Fe_2B layer thickness increased with the treatment time at 1173 K. The value of Fe_2B layer thickness ranged from 41.93 ± 8.25 µm for 2 h to 95.48 ± 17.4 µm for 8 h at 1173 K.

Figure 5 gives the SEM micrographs of the boride layers formed on the AISI S1 steels at increasing temperatures and for an exposure time of 4 h. The (boride layer/substrate) interface exhibited a saw-tooth morphology. The kinetics of formation of boride layers is a thermally activated phenomenon with a change in the layer thickness with increasing temperatures.

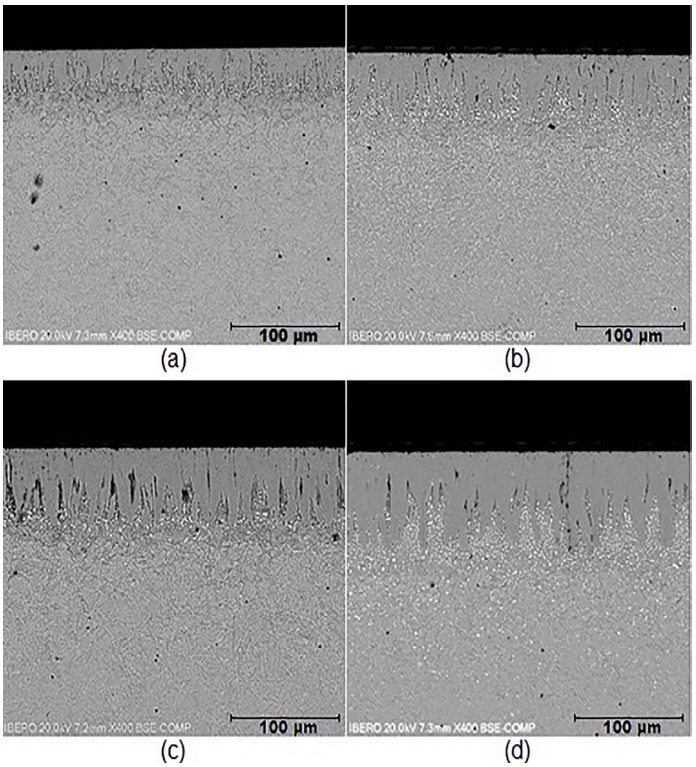

Figure 4. SEM micrographs of the cross-sections of borided AISI S1 steels at 1173 K during different exposure times: (a) 2 h, (b) 4 h, (c) 6 h, and (d) 8 h

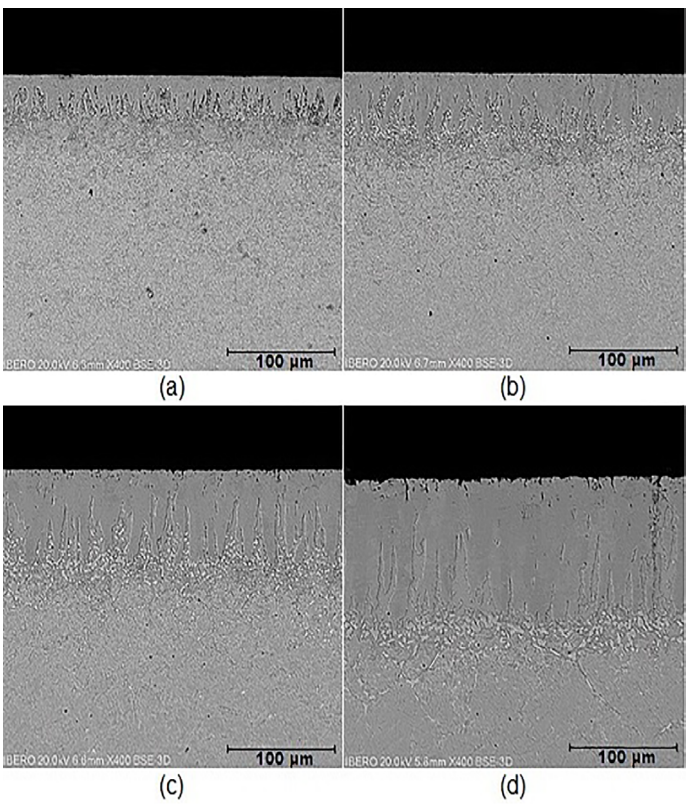

Figure 5. SEM micrographs of the cross-sections of AISI S1 steels borided with exposure time of 4 h, during different boriding temperatures: (a) 1123 K, (b) 1173 K, (c) 1223 K and (d) 1273 K

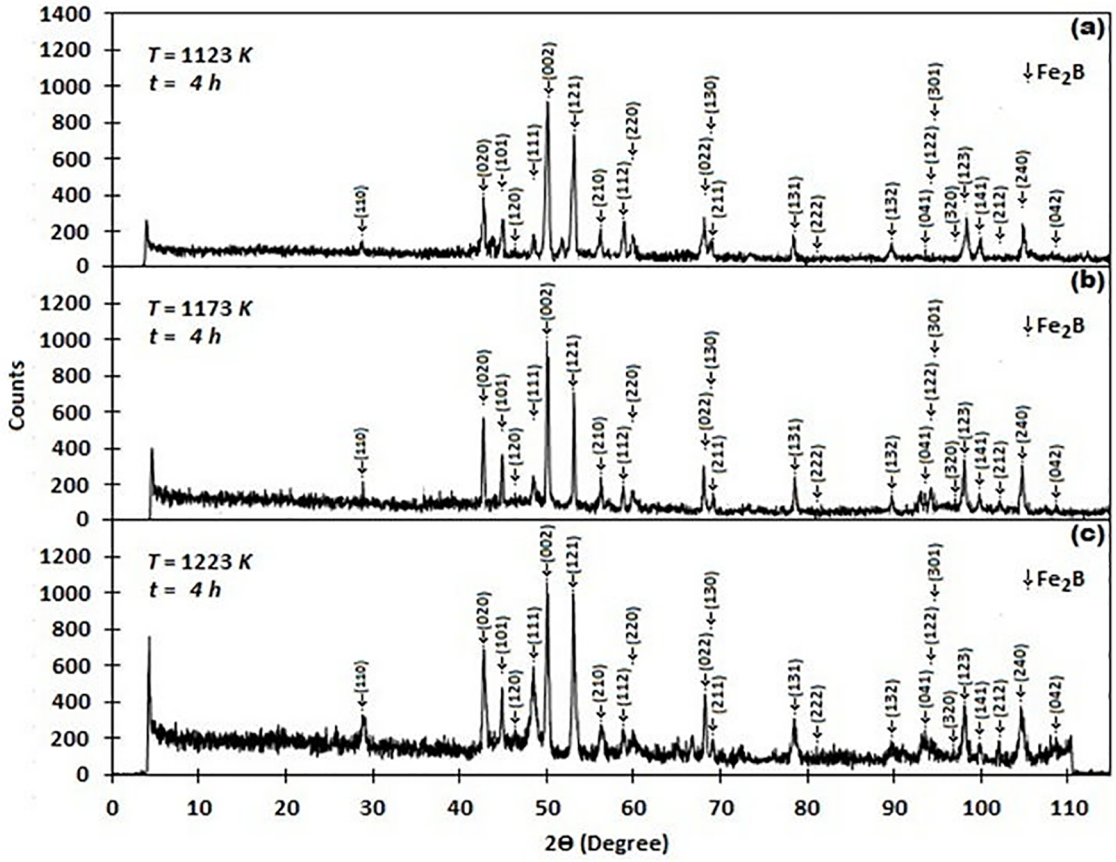

Figure 6. XRD patterns obtained at the surface of borided AISI S1 steels for three boriding conditions: (a) 1123 K for 4 h, (b) 1173 K for 4 h and (c) 1223 K for 4 h

4.2 XRD analysis

Figure 6 shows the XRD patterns obtained at the surface of borided AISI S1 steels at 1123, 1173 and 1223 K for 4 h of treatment. The XRD patterns revealed the presence of diffracting peaks belonging to the Fe_2B phase. The formation of Fe_2B layer is related to the quantity of active boron present in the boriding agent. The observed difference in the diffracted intensities can be explained by the textured growth along the easiest crystallographic direction 001 that minimizes the growth stress[20].

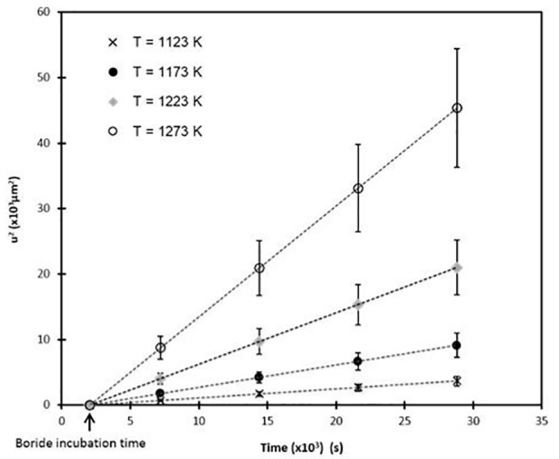

Figure 7. Square of boride layer thickness as a function of boriding time for increasing temperatures

4.3 Estimation of boron activation energy in AISI S1 steel

The experimental results are needed to evaluate the values of boron diffusion coefficients in Fe_2B in the temperature range 1123-1273 K by plotting the variation of the square of Fe_2B layer thickness as a function of treatment time. The intercept with the time axis yields the value of boride

Table 2. Experimental values of parabolic growth constants at the (Fe_2B/substrate) interface along with the corresponding boride incubation times.

T (K)	Experimental parabolic growth constant k ($\mu m \cdot s^{-0.5}$)	Boride incubation time $t_0^{Fe_2B}(T)$(s)
1123	0.3704	2038.8
1173	0.5837	2039.4
1223	0.8861	2040.2
1273	1.3016	2038.4

incubation time. Figure 7 gives the evolution of the square of Fe_2B layer thickness as a function of time for increasing values of boriding temperatures. The growth kinetics of Fe_2B layers is governed by the parabolic growth law. The slope of each straight line depicted in the Figure 7 represent the square of parabolic growth constant at each boriding temperature.

The experimental values of parabolic growth constants at the (Fe_2B/substrate) interface along with the corresponding boride incubation times are shown in Table 2.

It is seen that the values of boride incubation times are nearly constant. The following reason can be provided for this experimental observation. According to the design of the thermochemical treatment, the container is always placed at ambient temperature in a conventional furnace under a pure argon atmosphere until the boriding temperature (1123 K ≤ T ≤ 1273 K), the boride incubation time $t_0^{Fe_2B}$ will not depend on the boriding temperature in this early stage of the growth. The Fe_2B crystals grow from the contact zones between the metal surface and mixture of powders composed of 20% B_4C, 10% $KBF_4$and 70% SiC, lengthening upon the surface of the base metal forming a thin layer during the nucleation stage. For example, if you want to select T = 1273 K in the electronic control of the furnace, the thermochemical treatment will first reach the temperature of 1123 K at the same time as if you had selected the temperature of 1223 K, for this reason the boride incubation time will be a constant for each substrate.Figure 8 gives the temperature dependence of the boron diffusion coefficients in the Fe_2B layers following the Arrhenius equation.

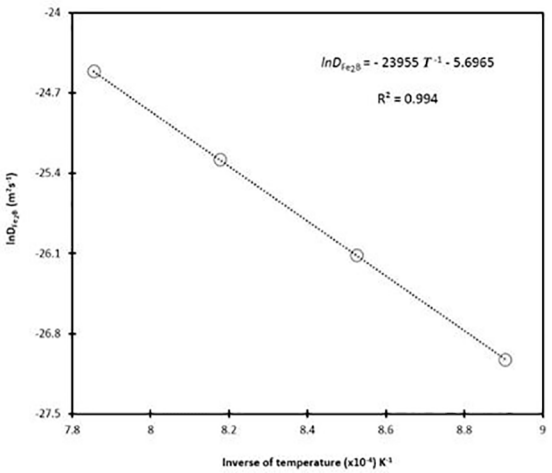

Figure 8. The temperature dependence of boron diffusion coefficient in the Fe_2B layer.

The value of boron diffusion coefficient in Fe_2B at each temperature was estimated from Equation (14) based on the integral method. This value can be easily obtained from the slope of straight line shown in Figure 8. The value of 199.16 $kJmol^{-1}$ indicates the amount of energy for the boron mobility in the easiest path corresponding to the crystallographic direction [001] along the Fe_2B layer. Therefore, the expression describing the evolution of boron diffusion coefficients in Fe_2B versus temperature is given by Equation (17) in the temperature range 1123-1273 K:

$$D_{Fe_2B} = 3.4 \times 10^{-3} \exp\left(\frac{-199.16 kJmol^{-1}}{RT}\right) \quad (17)$$

where R = 8.314 J mol^{-1} K^{-1} and *T* the absolute temperature in Kelvin.

Table 3 shows a comparison between the values of activation energy for boron diffusion in Armco iron and some ferrous alloys (steels and gray cast iron) and the estimated value of activation energy for boron diffusion in AISI S1 steel[3,12,21-28].

It is observed that the obtained values of boron activation energy by different investigators are dependent on several factors such as: (the method of calculation, the boriding method, the nature of boriding agent, the chemical reactions involved and the chemical composition of the substrate.

For example, Şeşen et al.[21] have borided an interstitial free (IF) steel by using the electrochemical boriding under

Table 3. Comparison of activation energy for boron diffusion in AISI S1 steel with other borided materials.

Material	Boriding method	Activation energy for boron diffusion (kJ mol^{-1})	References
XC38 steel	Liquid boriding	207.8 (Fe_2B)	12
IF steel	Electrochemical boriding	80.70-100.16 (FeB + Fe_2B) depending on the current density	21
AISI D2 steel	Salt-bath	170.0 (FeB + Fe_2B)	22
Q235 steel	Plasma electrolytic boriding	186.17(FeB + Fe_2B and Ni borides as precipitates)	23
AISI 316	Plasma paste boriding	250.8 (FeB + Fe_2B)	24
AISI 1018 Steel	Paste	159.3 (Fe_2B)	25
Armco Iron	Powder	157.5 (Fe_2B)	26
AISI 9840 steel	Powder	193.08 (Fe_2B)	27
EN-JL-250 Gray cast iron	Powder	134.21 (FeB + Fe_2B)	28
AISI P20 steel	Powder	200 (Fe_2B)	3
AISI S1 steel	Powder	199.16 (Fe_2B) by the integral method 199.1 (Fe_2B) by the masse balance equation	This work

different current densities. They produced a double boride layer (FeB and Fe_2B) where FeB was a dominant phase. A metastable iron boride was also identified by XRD analysis.

The calculated boron activation energies ranged between 80.70 and 100.16 kJ mol^{-1}, depending on the value of current density in the range 0.1 -0.4 A cm^{-2}. It is noticed that these values are lower than those obtained from other reported works[3,12,21-28]. It should be attributed to the absence of carbon and nitrogen as interstitial atoms leading to the increase in the boron mobility within the material substrate. In addition, the estimated value of activation energy for boron diffusion in AISI S1 steel is very comparable to the values estimated for AISI 9840 and AISI P20 steels by using the same chemical composition of boriding agent[3,27].

4.4 Experimental validation of different diffusion models

To experimentally validate the diffusion model based on the integral method and four diffusion models, three extra boriding conditions were used for this purpose. Figure 9 gives the SEM images of the cross-sections of Fe_2B layers formed at 1173 K for 3.5 h and 6.5 h and at 1223 K for 1.5 h, respectively.

For such boriding conditions, a compact single phase layer of Fe_2B was produced with a saw-tooth morphology. On the basis of integral method, the expression of Fe_2B layer thickness depending on the boriding parameters (time and temperature) is given by Equation (18):

$$u(t) = \sqrt{\frac{D_{Fe_2B}\left[t - t_0^{Fe_2B}(T)\right]}{\eta}} \tag{18}$$

with $D_{Fe_2B} = D_0 \exp\left(-\frac{Q}{RT}\right)$ and η=13.3175

where Q is the activation energy for boron diffusion (kJmol^{-1}), D_0 represents a pre-exponential constant (m^2 s^{-1}) and T is the absolute temperature in Kelvin.

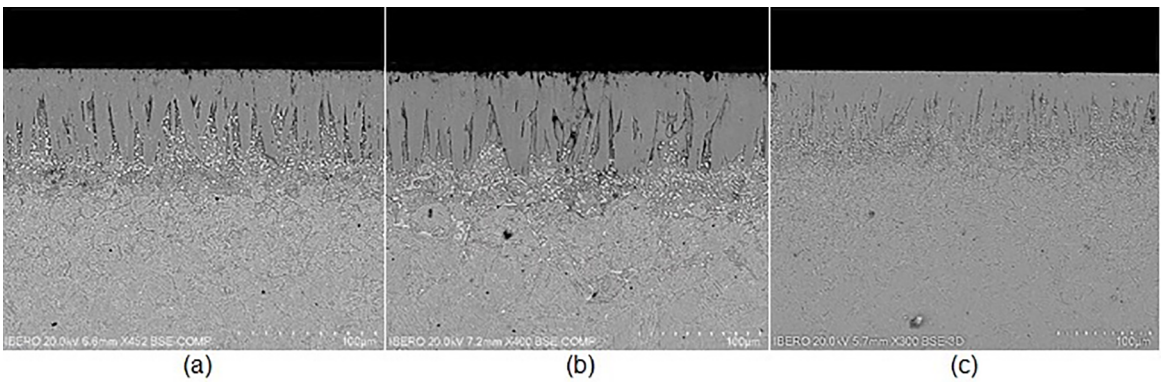

Figure 9. SEM micrographs of the boride layers formed at the surfaces of AISI S1 steel for three extra boriding conditions: (a) 1173 K for 3.5 h, (b) 1173 K for 6.5 h and (c) 1223 K for 1.5 h

Table 4. Values of boron activation energies estimated from all diffusion models with the expressions used to estimate the Fe_2B layer thickness.

D0 (m^2s^{-1})	Activation energy Q (kJmol^{-1})	Equations for evaluating the Fe_2B layer thickness	References
5.9×10^{-3}	199.15	$u(t) = \sqrt{\frac{8D_{Fe_2B}(C_{up}^{Fe_2B} - C_{low}^{Fe_2B})t}{\ln\left(\frac{t}{t_0^{Fe_2B}}\right)(C_{up}^{Fe_2B} + C_{low}^{Fe_2B} - 2C_0)}}$	5
5.9×10^{-3}	199.15	$u(t) = 2\varepsilon\sqrt{D_{Fe_2B}t}$ with ε=0.0975	6
5.9×10^{-3}	199.15	$u(t) = 2\sqrt{\frac{D_{Fe_2B}t}{\pi}}\frac{(C_{up}^{Fe_2B} - C_{low}^{Fe_2B})\exp(-\beta^2k^2/4D_{Fe_2B})\beta^2}{[0.5(C_{up}^{Fe_2B} + C_{low}^{Fe_2B}) - C_0]erf\left(\frac{k\beta}{2\sqrt{D_{Fe_2B}}}\right)}$ with β=0.9517	7
5.9×10^{-3}	199.15	$u(t) = 2\sqrt{\frac{D_{Fe_2B}(C_{up}^{Fe_2B} - C_{low}^{Fe_2B})t}{(C_{up}^{Fe_2B} + C_{low}^{Fe_2B} - 2C_0)}}$	8
3.4×10^{-3}	199.16	$u(t) = \sqrt{\frac{D_{Fe_2B}\left[t - t_0^{Fe_2B}\right]}{\eta}}$ with η=13.3175	Present work

Table 5. Comparison between the experimental values of Fe_2B layers' thicknesses (obtained for three boriding conditions) and the predicted values using different models for an upper boron content in the Fe_2B phase equal to 9 wt.%.

Boriding conditions	Experimental value (μm)	Simulated value (μm)[5]	Simulated value (μm)[6]	Simulated value (μm)[7]	Simulated value (μm)[8]	Simulated value (μm) Equation (18)
1173 K for 3.5 h	59.65±10.43	57.00	61.84	55.37	61.94	60.37
1173 K for 6.5 h	75.14 ±13.76	77.68	84.28	75.45	84.41	85.86
1223 K for 1.5 h	61.54±11.45	56.64	6146	55.02	61.55	51.71

Table 4 provides the expressions of Fe_2B layer thickness as a function of boriding parameters derived for four diffusion models with Equation (18) valid for the integral method. It is seen that the estimated value of boron activation energy for AISI S1 steel by using the diffusion model[6] is very close to that obtained from the integral method.

Table 5 gives a comparison between the experimental values of Fe_2B layers' thicknesses (obtained for three boriding conditions) and the predicted values using four different models and the integral method for an upper boron content in the Fe_2B phase equal to 9 wt.%.

It is seen that the experimental values in terms of Fe_2B layers' thicknesses coincide in a satisfactory way with the predicted results.

Equation (18) can be employed as a simple tool to predict the optimum value of Fe_2B layer thickness as a function of boriding parameters (the treatment time and the process temperature) as shown in Figure 10 to match the case depth that meets requirements for a practical use of AISI S1 steel in the industry.

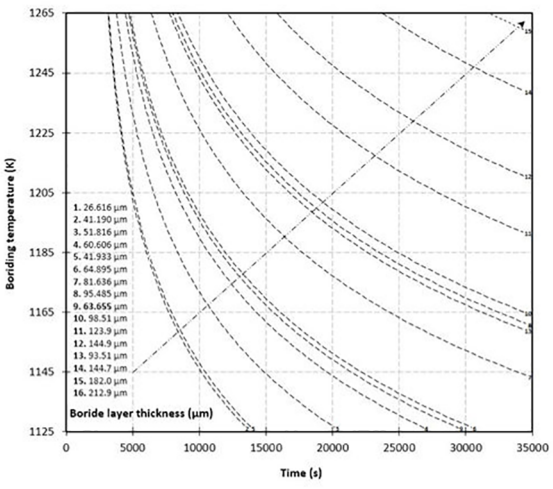

Figure 10. Iso-thickness diagram describing the evolution of Fe_2B layer thickness as a function of boriding parameters

5. Conclusions

In this current work, the AISI S1 steel was treated by the powder-pack boriding in the temperature range 1123-1273 K with a variable treatment time (from 2 h to 8 h). The boriding agent was composed of 20% B_4C, 10% KBF_4 and 70% SiC. The XRD analysis confirmed the presence of Fe_2B phase in the boride layer for all boriding conditions. For indication, the XRD patterns for the borided samples at 1123, 1173 and 1223 K for 4 h were only shown as experimental evidence. The SEM examinations revealed a saw- tooth morphology for the Fe_2B layers formed on AISI S1 steel. The growth kinetics of Fe_2B layers on AISI S1 steel was described by the classical parabolic growth law with the occurrence of a constant boride incubation time. The value of activation energy for boron diffusion in AISI S1 steel was estimated as 199.16 $kJmol^{-1}$ on the basis of the integral method,and compared with that obtained from an alternative diffusion model. Furthermore, this value of boron activation energy was compared to the values found in the literature. The present kinetic approach based on the integral method and four diffusion models were experimentally validated by using three extra boriding conditions. As a consequence, a good agreement was noticed between the experimental values of Fe_2B layers' thicknesses and the predicted thicknesses. Finally, an iso-thickness diagram was suggested to be used as a simple tool for selecting the optimized value of Fe_2B layer thickness for practical use of AISI S1 steel in the industry.

6. Acknowledgements

The work described in this paper was supported by a grant of PRDEP and CONACyT México (National Council of Science and Techonology). Likewise, FCS reconoce los fondos del Departamento de Física y Matemáticas y de la División de Investigación de la UIA.The authors wish to thank to the Laboratorio de Microscopía de la UIA.

7. References

1. Sinha AK. Boriding (Boronizing) of Steels. In: *ASM Handbook. Volume 4. Heat Treating*. Materials Park: ASM International; 1990. p. 437-447.
2. Keddam M, Chentouf SM. A diffusion model for describing the bilayer growth (FeB/Fe2B) during the iron powder-pack boriding. *Applied Surface Science*. 2005;252(2):393-399.
3. Keddam M, Elias-Espinosa M, Ortiz-Domínguez M, Simón-Marmolejo I, Zuno-Silva J. Pack-boriding of AISI P20 steel: Estimation of boron diffusion coefficients in the Fe_2B layers and tribological behaviour. *International Journal of Surface Science and Engineering*.2017;11(6):563-585.
4. Keddam M, Ortiz-Dominguez M, Elias-Espinosa M, Arenas-Flores A, Zuno-Silva J, Zamarripa-Zepeda D, et al.Kinetic Investigation and Wear Properties of Fe_2B Layers on AISI 12L14 Steel. *Metallurgical and Materials Transactions* A.2018;49(5):1895-1907.
5. Ortiz-Domínguez M, Flores-Rentería MA, Keddam M, Elias-Espinosa M, Damián-Mejía O, Aldana-González JI, et al. Simulation of growth kinetics of Fe_2B layers formed on gray cast iron during the powder-pack boriding. *Materials and Technology*. 2014;48(6):905-916.
6. Elias-Espinosa M, Ortiz-Domínguez M, Keddam M, Gómez-Vargas OA, Arenas-Flores A, Barrientos-Hernández FR, et al. Boriding kinetics and mechanical behaviour of AISI O1 steel. *Surface Engineering*. 2015;31(8):588-597.
7. Nait Abdellah Z, Keddam M, Chegroune R, Bouarour B, Haddour L, Elias A. Simulation of the boriding kinetics of Fe_2B layers on iron substrate by two approaches. *Matériaux et Techniques*. 2012;100(6-7):581-588.
8. Flores-Rentería MA, Ortiz-Domínguez M, Keddam M, Damián-Mejía O, Elias-Espinosa M, Flores-González MA, et al. A Simple Kinetic Model for the Growth of Fe_2B Layers on AISI 1026 Steel During the Powder-pack Boriding. *High Temperature Materials and Processes*. 2015;34(1):1-11.
9. Kouba R, Keddam M,Kulka M. Modelling of paste boriding process. *Surface Engineering*. 2015;31(8):563-569.
10. Ramdan RD, Takaki T, Tomita Y. Free Energy Problem for the Simulations of the Growth of Fe_2B Phase Using Phase-Field Method. *Materials Transactions*.2008;49(11):2625-2631.
11. Campos I, Oseguera J,Figueroa U, Garcia JA, BautistaO, Kelemenis G. Kinetic study of boron diffusion in the paste-boriding process. *MaterialsScience and Engineering: A*. 2003;352(1-2):261-265.
12. Mebarek B, Benguelloula A, Zanoun A. Effect of Boride Incubation Time During the Formation of Fe_2B Phase. *Materials Research*. 2018;21(1):e20170647.DOI: http://dx.doi.org/10.1590/1980-5373-mr-2017-0647
13. Brakman CM, Gommers AWJ,Mittemeijer EJ. Boriding of Fe and Fe-C, Fe-Cr, and Fe-Ni alloys; Boride-layer growth kinetics. *Journal of Materials Research*. 1989;4(6):1354-1370.
14. Yu LG, Chen XJ, Khor KA, Sundararajan G. FeB/Fe_2B phase transformation during SPS pack-boriding: boride layer growth kinetics. *Acta Materialia*.2005;53(8):2361-2368.
15. Okamoto H. B-Fe (boron-Iron). *Journal of Phase Equilibria and Diffusion*. 2004;25(3):297-298.
16. Krukovich MG, Prusakov BA, Sizov IG. The Components and Phases of Systems 'Boron-Iron' and 'Boron-Carbon-Iron'.In: Krukovich MG, Prusakov BA, Sizov IG. *Plasticity of Boronized Layers. Volume 237 of the Springer Series in Materials Science*. Cham: Springer; 2016. P. 13-21.
17. Goodman TR. Application of Integral Methods to Transient Nonlinear Heat Transfer. *Advances in Heat Transfer*.1964;1:51-122.
18. Reséndiz-Calderon CD, Rodríguez-Castro GA, Meneses-Amador A, Campos-Silva IE, Andraca-Adame J, Palomar-Pardavé ME, et al. Micro-Abrasion Wear Resistance of Borided 316L Stainless Steel and AISI 1018 Steel. *Journal of Materials Engineering and Performance*. 2017;26(11):5599-5609.
19. Carbucicchio M, Badani L,Sambogna G. On the early stages of high purity iron boriding with crystalline boron powder. *Journal of Materials Science*. 1980;15(6):1483-1490.
20. Palombarini G, Carbucicchio M. Growth of boride coatings on iron. *Journal of Materials Science Letters*. 1987;6(4):415-416.
21. Sesen FE, ÖzgenÖS, Sesen MK. A Study on Boronizing Kinetics of an Interstitial-Free Steel. *Materials Performance and Characterization*. 2017;6(4):492-509.
22. Sen S, Sen U,Bindal C. An approach to kinetic study of borided steels. *Surface and CoatingsTechnology*. 2005;191(2-3):274-285.
23. Jiang YF, BaoYF, Wang M. Kinetic Analysis of Additive on Plasma Electrolytic Boriding. *Coatings*. 2017;7(5):61.
24. Chegroune R, Keddam M, Nait Abdellah Z, Ulker S, Taktak S, Gunes I. Characterization and kineticsof plasma-paste-borided AISI 316 steel. *Materials and Technology*. 2016;50(2):263-268.
25. Campos-Silva I, Ortiz-Dominguez M. Modelling the growth of Fe_2B layers obtained by the paste boriding process in AISI 1018 steel irons. *International Journal of Microstructure and Materials Properties*. 2010;5(1):26-38.
26. Elias-Espinosa M, Ortiz-Domínguez M, Keddam M, Flores-Rentería MA, Damián-Mejía O, Zuno-Silva J, et al. Growth Kinetics of the Fe_2B Layers and Adhesion on Armco Iron Substrate. *Journal of Materials Engineering and Performance*. 2014;23(8):2943-2952.
27. Ortiz-Domínguez M, Gómez-Vargas OA, Keddam M, Arenas-Flores A, García-Serrano J. Kinetics of boron diffusion and characterization of Fe_2B layers on AISI 9840 Steel. *Protection of Metals and Physical Chemistry of Surfaces*. 2017;53(3):534-547.
28. Azouani O, Keddam M, Allaoui O, Sehisseh A. Kinetics of the Formation of Boride Layers on EN-GJL-250 Gray Cast Iron. *Materials Performance and Characterization*. 2017;6(4):501-522.